

Dilute Al and V NMR in α -Ti

L. H. Chou* and T. J. Rowland

Department of Materials Science and Engineering, University of Illinois at Urbana-Champaign, Urbana, Illinois 61801

(Received 20 May 1991)

We report a nuclear-magnetic-resonance investigation of four titanium alloys: Ti-1 at. % V, Ti-2 at. % V, Ti-1 at. % Al, and Ti-2 at. % Al. Interpretation of the experimental ^{51}V and ^{27}Al absorption curves was accomplished largely by comparison with computer-simulated curves. Since the latter include the effects of nuclear-quadrupole and anisotropic Knight-shift interactions, dipolar broadening, and inhomogeneous Knight shift for the V and Al solute nuclei, the comparison yields experimental values for the electric-field gradient, axially symmetric anisotropic Knight shift, and isotropic Knight shift, from which we attempt to deduce the local charge distribution at the V or Al atoms in the hcp α -Ti matrix. We find that the localized states on an Al impurity exhibit very little of the character of the host Ti atomic structure. There is no orbital contribution to the Knight shift and the s conduction-electron density at Al sites is small. On the other hand, when vanadium is present as a dilute solute in the Ti lattice, only minor changes in its Knight shift are found. There is a large orbital-shift contribution, and the V nuclear absorption exhibits much the same character as in pure metallic V; there is, however, clear evidence of the V charge distribution assuming the hexagonal symmetry of the Ti lattice. The measured temperature dependences of the anisotropic Knight shift and electric-field-gradient values at V solute sites in Ti are also discussed. On partitioning the field gradient we find that the contribution from local non- s electrons is about two to five times larger in magnitude than the Ti-lattice ion value, a strong indication that the electronic structure near V (but not Al) resembles that of the matrix Ti.

I. INTRODUCTION

The object of this investigation is to compare the local electronic structure of a simple metal (Al) to that of a transition metal (V) at low concentration in a transition-metal (Ti) matrix. Despite certain drawbacks nuclear magnetic resonance (NMR) is used to investigate the magnitude and symmetry of the charge-density distribution around the solute nucleus. Much of the previous experimental work has centered on the band structure of alloys,¹⁻⁴ while relatively little has been devoted to the study of the localized bonding of solute atoms in a transition-metal matrix.⁵ Most of the band-structure studies of alloy systems were done by specific-heat measurement, which showed a linear dependence on valence Z only. Stern proposed a rigid-band model³ to explain the linear response. This model assumed an unchanged density-of-states curve of an alloy from its pure host; the addition of foreign atoms with a different valence from the host was thought to change the position of the host Fermi level E_F . Succeeding work¹ showed this model to be incorrect. The low-temperature electronic specific-heat data of dilute alloys included changes related to the local electronic charge density at E_F near the impurity.

The presence of both the electric-field gradient (EFG) and the axially anisotropic Knight shift K_{ax} has been detected in several pure hcp metals, such as Sc, Y,⁶ and La,⁷ but there is no reported work on corresponding alloy systems. This paper describes the observation of these combined effects at solute sites in alloys. The detection and measurement of both the electric-field gradient and anisotropic Knight shift at the solute site lends a clear

advantage in deducing the local charge configuration. Other techniques, such as the Mössbauer effect, pure nuclear quadrupole resonance, and γ - γ time differential perturbed angular correlation, can measure only the electric-field gradient.

The alloys of interest here are the hexagonal-close-packed substitutional solid solutions of Ti with solute concentration of 1 or 2 at. % Al or V. (Pure Al is fcc, pure V is bcc.) The solute concentrations were kept low in an attempt to stay within the α -Ti phase region in the temperature range of interest,^{8,9} and to increase the probability that each solute atom would have no nearest-neighbor solutes, and thus experience identical and symmetric local surroundings. The dipole-dipole interaction of solute and solvent nuclei broaden the solute NMR line. Only about 13% of the Ti matrix nuclei have nonzero spin; the dipolar broadening of the solute line by the Ti nuclei is thus very small. Most of the solute linewidth is caused by the distribution of local electron charge. We can thus obtain information about the local charge distribution near the solute atom from an analysis of the absorption line position and shape. The interpretation of the data includes the effects of nuclear quadrupole interaction, anisotropic Knight shift, dipolar broadening, and inhomogeneous Knight-shift distribution at the solute sites.

II. EXPERIMENTAL PROCEDURE

The samples used in the present work were filings of Ti alloys. Iodide titanium was used as the solvent for preparing the alloys. The solute metals V and Al had a nom-

inal metallic purity of 99.9% and 99.999%, respectively. All the alloys were prepared by arc melting under purified argon. Each specimen was homogenized at 1280°C for about 3 days. The solute composition was found to vary by about ± 0.02 at. % from its mean value according to the results of microprobe analysis. The sample used was in the form of filings. The latter were prepared by means of an automatic filing machine and sieved to provide samples of 200 mesh and finer; these were annealed at 700°C for about 3 days to remove the cold work introduced through the filing process. Lattice distortion resulting from filing alters the electric-field gradient at V or Al nuclei and is a source of line broadening. All of the heat treatments were carried out in Mo thimbles in evacuated quartz capsules which were air cooled following annealing. X-ray diffraction was used to verify the crystal structure. See also Sec. IV E.

For reasons that will be explained later, two techniques were used for the measurements. The steady-state crossed-coil NMR detection technique was used for the Ti-V samples; a pulse technique was used for the Ti-Al alloys. The nuclear-magnetic-resonance apparatus and associated equipment was of standard design. For work on ^{51}V in Ti, a modulation frequency of 76 Hz was used; the modulation field was parallel to the external applied field. A Fabri-Tek 1070 series signal averager having 1024 channels was used to record from 256 to 1024 field sweeps for each resonance curve observed.

For ^{51}V data taken below 8 MHz, the weak ^{51}V resonance was on the wing of the very large ^{27}Al resonance from the wall of the probe being used. In order to study the ^{51}V it was necessary to greatly attenuate the probe ^{27}Al resonance. Silver foil was placed between the quartz tube, which held the transmitter and receiver coils and the solid aluminum alloy probe body. Foil 127 μm thick was used for the 4–8-MHz probe; two 127- μm -thick foils were used to line the 2–4-MHz probe wall. The transmitter-receiver setup used was capable of working to 29 MHz. The reference used for the Knight-shift mea-

surements was the ^{51}V resonance (or ^{23}Na resonance at 29 MHz) in a saturated aqueous sodium metavanadate solution. For ^{27}Al the resonance in a saturated aqueous aluminum chloride solution was used. The Ti-V work was done at room temperature and liquid-nitrogen temperature; all the Ti-Al work was done at room temperature.

III. EXPERIMENTAL RESULTS

A. Ti-V alloys

By comparing the ^{51}V nuclear absorption intensity of the Ti-2 at. % V sample and pure vanadium filings, it was concluded that only the central line contributed to the solute ^{51}V resonance. The subsequent detection of ^{51}V satellite peaks in the Ti-1 at. % V and Ti-2 at. % V samples at 29 MHz, as shown in Fig. 1, confirmed the view that the absorption near $\nu = \nu_0$ could be attributed to the $m = -\frac{1}{2} \rightarrow \frac{1}{2}$ transition alone. This result plays an important part in line-shape analysis.

The ^{51}V resonance line shape and linewidth vary with frequency; further, data taken early in this study showed that the peak-to-peak derivative linewidth δH_{pp} at 8 MHz is about five times greater than the calculated dipolar value. The quantity δH_{pp} for two different Ti-V compositions at several frequencies are tabulated in Table I. For both concentrations, δH_{pp} has its minimum at about 5 MHz. We note here that a combined positive anisotropic Knight shift and quadrupole interaction leads to a minimum in the linewidth at an intermediate field. At high field the Knight shift dominates the line shape while at low field the quadrupole interaction dominates.¹⁰ The change is very pronounced within the frequency range covered in this work. At 29 MHz, the width and shape are characteristic of a positive anisotropic Knight shift; at 4 MHz and lower frequencies, second-order quadrupole broadening of the central line becomes increasingly

TABLE I. Room-temperature experimental and calculated peak-to-peak linewidth δH_{pp} of Ti-1 at. % V and Ti-2 at. % V samples at several frequencies are tabulated. Experimental peak-to-peak linewidth δH_{pp} of Ti-1 at. % Al and Ti-2 at. % Al samples at 29, 94, and 130 MHz are also shown. Linewidths δH_{pp} are given in units of Oe.

ν_0 (MHz)	Ti-1 at. % V		Ti-2 at. % V		Ti-1 at. % Al	Ti-2 at. % Al
	δH_{pp} (Oe) (expt.)	δH_{pp} (Oe) (calc.)	δH_{pp} (Oe) (expt.)	δH_{pp} (Oe) (calc.)	δH_{pp} (Oe) (expt.)	δH_{pp} (Oe) (expt.)
2			11.0 ^a	11.1		
2.75			7.6 \pm 0.6	8.11		
3			6.7 ^a			
3.5			6.2 ^a			
3.78	4.9 \pm 0.1	5.24	5.2 \pm 0.3	5.28		
5.0	3.8 \pm 0.4	3.67	4.3 \pm 0.2	4.33		
8.0	3.9 \pm 0.3	4.10	4.9 \pm 0.3	4.86		
16.0	12.9 \pm 0.8	13.44	13.3 \pm 0.5	13.18		
29	23.2 \pm 0.1	22.97	23.2 \pm 1.2	22.85	5.5	5.6
94					8.5 ^b	9.0 ^b
130					11.3 ^b	12.4 ^b

^aThere is no error bar because only one piece of data was taken.

^bObtained using the pulse technique; see the text.

apparent. The presence of these effects precludes the uncritical use of the derivative zero in defining the resonance position ν_0 .

Computer simulation of the absorption was required in order to proceed. This was done by extending the work of Jones, Graham, and Barnes.¹⁰ Numerical calculations of line shape were done using the following conditions: (i) the solute site is treated as having axial symmetry for both the anisotropic Knight shift and electric-field gradient; (ii) symmetric broadening is introduced and represented by a Gaussian function whose width is independent of angular orientation and external field; (iii) a distribution of isotropic Knight shifts represented by a Gaussian of fixed width in percent is introduced, i.e., the width of this distribution is proportional to H_0 . Any distribution in anisotropic Knight shift is neglected.

By varying the parameters associated with the breadth and shape of the absorption together with their field dependences, we construct simulated lines which agree very well with those of the experimentally recorded lines (cf. Fig. 2). The parameters used for the simulation of our room-temperature lines are $a = K_{ax}/(1 + K_{iso}) = 0.00029$, and $\nu_Q = 93.3$ kHz. The latter is the line splitting of the first satellite line pair ($m = \frac{3}{2} \rightarrow \frac{1}{2}$, $m = -\frac{1}{2} \rightarrow -\frac{3}{2}$) in terms of frequency. To take account of the distribution in Knight shift, a Gaussian with a full width $2\langle(\Delta K)^2\rangle^{1/2}$ of 0.004% is used. Here, ΔK is simply $(K - K_0)$. For liquid-nitrogen temperature results, the parameters used for the simulation are $a = 0.00039$ and $\nu_Q = 108$ kHz. A Gaussian distribution of K_{iso} with a width of 0.005% was used. The isotropic Knight shift is found to be 0.54% for both temperatures.

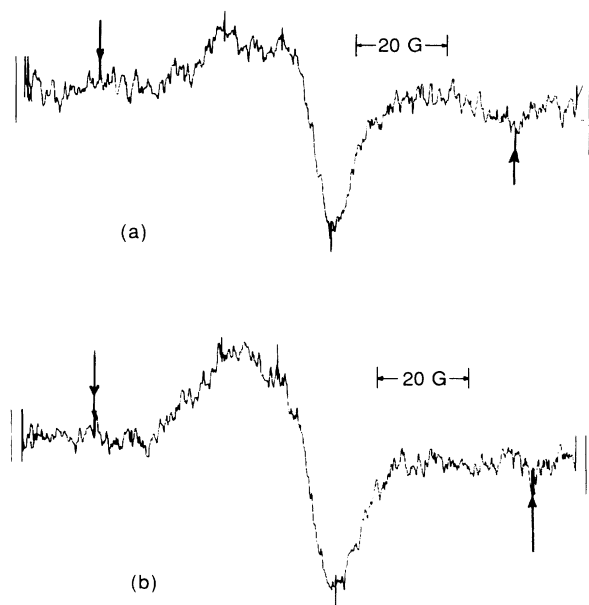


FIG. 1. The first satellite pair $m = \frac{3}{2} \rightarrow \frac{1}{2}$ (arrows) of (a) Ti-1 at. % V and (b) Ti-2 at. % V. Magnetic-field calibration is indicated; field increases to the right. Frequency $\nu_0 = 28.9$ MHz.

B. Ti-Al alloys

The Ti-Al room-temperature measurements were done at three different frequencies: 29, 94, and 130 MHz. The steady-state technique was used at 29 MHz and the pulse technique at 94 and 130 MHz.

In order to make a direct comparison between Ti-V and Ti-Al alloys, the measurements for both solutes ideally should have been done at the same frequencies, but due to the great width of the ^{51}V resonance at 8.4 and 11.7 kOe and the interference of the background probe ^{27}Al resonance with the ^{27}Al of our sample at low field, it could not be done. The ^{51}V resonance has an estimated linewidth of 75 Oe (84 kHz) and 105 Oe (118 kHz) at 94

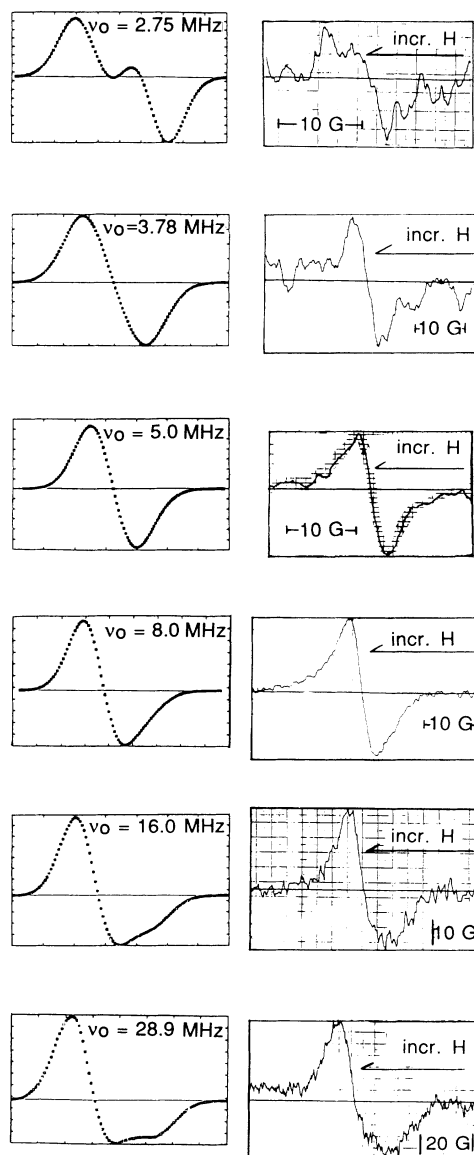


FIG. 2. The room-temperature experimental ^{51}V absorption derivative lines of Ti-2 at. % V alloys and corresponding computer simulated lines. Direction of external field sweep, ^{51}V resonance frequency, and external field calibration are shown.

and 130 MHz, respectively. The superconducting magnet spectrometer system used at these two frequencies has a window of 140 kHz at both 94 and 130 MHz. This window is not wide enough to allow undistorted detection of the whole ^{51}V resonance central line in the Ti-V alloys.

The crossed-coil technique was applied to the Ti-Al alloys at 29 MHz only. At 16 MHz, two ^{27}Al resonance centers (one from the sample and another from the probe) were only 16 Oe apart, and no quantitative analysis was done. At 8 MHz and lower frequencies the result could not be meaningfully analyzed because of the poor signal-to-noise ratio and the interference of the ^{27}Al resonance from the probe even with Ag foil lining.

The linewidths δH_{pp} of ^{27}Al in the Ti-Al alloy samples at each frequency are listed in Table I. At 130 MHz, linewidths of about 12 Oe were obtained. The broadening caused by an inhomogeneous Knight shift dominates at this high frequency. Due to the limited number of data points (three for each Ti-Al sample), the absolute simulation is difficult. The line simulation and fitting program requires more data points. At best, we found the magnitude of $r = a\nu_0^2/b$, where $b = \frac{1}{64}\nu_Q(2I+3)(2I-1)$, to lie between 0.1 and 0.3 at 29 MHz. The sign of the anisotropic Knight shift cannot be determined but its magnitude is $(1.5 \pm 0.5) \times 10^{-5}$. The isotropic Knight shift is 0.031%; in addition, an inhomogeneous Knight-shift distribution of 0.008% was required to produce a good fit to the data. The first satellite pair splitting ν_Q is equal to (339 ± 6) kHz.

IV. DISCUSSION

An analysis of the Knight shift is given in Sec. IV A. In Sec. IV B we analyze the electric-field gradient. The rest of the discussion is on the effect of concentration, annealing, and some other possible line-broadening sources. The fact that we are dealing with real solid solutions rather than structures having an identical electronic configuration at each solute site complicates the interpretation.

A. Knight shift

The ^{51}V shift in pure V, and Ti-1 at. % V and the ^{27}Al Knight shift in pure Al, and Ti-1 at. % Al at three

different temperatures are listed in Table II. The respective Knight shifts were the same for 2 at. % as for 1 at. % solute concentration.

The Knight shift K of metals is usually regarded as composed of several independent contributions:

$$K = a\chi_s + b\chi_d + c\chi_{\text{orb}}, \quad (1)$$

where χ_s and χ_d are the spin paramagnetic susceptibilities of the electrons in the s and d bands and χ_{orb} is the orbital paramagnetism associated with the d band. The constants a , b , and c have values which depend on the electronic structure in the vicinity of the nucleus. The first term $a\chi_s$ results from the s electrons on the Fermi surface. For metal in an external field it causes a small magnetic field at the nucleus through the hyperfine contact interaction. The simple metals K and Cu which have only one s outer electron and filled core show a Knight shift of 0.26% and 0.24% for ^{39}K in pure K and ^{63}Cu in pure Cu, respectively. These Knight shifts are expected to result from hyperfine contact interaction only and are much smaller than the isotropic Knight shift of ^{51}V in pure bcc V ($\sim 0.58\%$) and of ^{51}V in dilute solution in hcp Ti. But the four elements K, Ti, V, and Cu are in the same row of the Periodic Table, and the two elements Ti and V have a free-atom outer structure of $3d^24s^2$ and $3d^34s^2$, respectively. The fact that the isotropic Knight shift of ^{51}V in pure V ($\sim 0.58\%$) and of ^{51}V in Ti ($\sim 0.54\%$) are much larger than those of ^{39}K in pure K ($\sim 0.26\%$) and ^{63}Cu in pure Cu ($\sim 0.24\%$) suggests that contributions other than, or in addition to, the hyperfine contact interaction are present at ^{51}V nuclei in bcc V, and at V in solution in hcp Ti. Titanium, which has an outer structure of $3d^24s^2$, has a high density of d states on the Fermi surface.¹¹ Vanadium, which has one more outer d electron than titanium, is expected to assume the charge-density distribution of the Ti because of the large d overlap when it is embedded in a Ti matrix. The result would be a negative contribution to the Knight shift caused by polarizing the core- s electrons.¹² In view of this we might expect the Knight shift of ^{51}V in V or Ti to be less than about 0.25%, much less than the observed K_{iso} ($\sim 0.54\%$) value. From Eq. (1), it is clear that the orbital term is significant. This shift results from the interaction of the nuclear spin with the orbital motion of the electrons in-

TABLE II. The isotropic Knight shift of ^{51}V in pure vanadium, and Ti-1 at. % V; and of ^{27}Al in pure aluminum, and Ti-1 at. % Al, at three different temperatures.

Metal	T (K)		
	298	77	$\cong 0$
Pure V	0.58% ^a	0.572% ^a	0.57% ^b
Ti-1 at. % V	$0.540 \pm 0.002\%$	$0.540 \pm 0.005\%$	
Pure Al	0.164% ^c	0.162% ^d	0 ^e
Ti-1 at. % Al	$0.031\% \pm 0.004\%$		

^aL. E. Drain, Proc. Phys. Soc. **83**, 755 (1964).

^bReference 14.

^cE. R. Andrew, W. S. Hinshaw, and P. S. Tiffen, Phys. Lett. **46A**, 57 (1973).

^dG. C. Carter, L. H. Bennett, and D. Kahn, *Progress in Materials Science* (Pergamon, Oxford, 1977), Vol. 20, p. 134.

^eR. H. Hammond and G. M. Kelly, Phys. Rev. Lett. **18**, 156 (1967).

duced by the applied magnetic field H . It gives rise to a second-order contribution. The occupied and unoccupied Bloch states are admixed by the application of the field H . The resulting admixture produces a field which interacts with the nucleus. A rough estimate of the magnitude of the orbital Knight shift is given by¹³

$$K_{\text{orb}} \approx \frac{n_i n_f \langle r^{-3} \rangle}{\Delta}, \quad (2)$$

where n_i and n_f are the numbers of occupied and unoccupied Bloch states, respectively, and Δ is the conduction-electron bandwidth. The primary contribution from the quantity $\langle r^{-3} \rangle$ arises from the d -band charge-density distribution. There is little or no temperature dependence in this term. Particularly strong orbital effects are expected in roughly half-filled d -band transition metals. The observed large positive K values of ^{51}V in V and Ti probably arise from the Knight-shift contribution from the temperature-independent orbital term first noted by Van Vleck. Its existence was confirmed in V metal by experiments in which the ^{51}V resonance was observed in the superconducting state.¹⁴ According to BCS theory¹⁵ of superconductivity, the spin susceptibility,¹⁶ and therefore the portion of the Knight shift depending upon spin, should vanish exponentially below T_c , the superconducting critical temperature. In V the Knight shift remains large ($\sim 0.57\%$) and positive as a result of the orbital contribution.

There is some evidence, both experimental¹⁷ and theoretical,¹⁸ that the atomic radius of V in Ti is larger than when it is in V. We have made a crude estimate of $\langle r^{-3} \rangle = 1.6 \times 10^{25} \text{ cm}^{-3}$ using an interpolation of Hartree Fock results;¹⁹ this is 13% smaller than $\langle r^{-3} \rangle$ for that of V in pure V. With the assumption that $n_i n_f / \Delta$ is about the same for V in Ti as for V in V, an orbital contribution to the Knight shift of V in Ti of 0.50% is obtained from Eq. (2). In view of the possible error in this estimate the observed Knight shift of ^{51}V in Ti is almost entirely orbital.

The ^{27}Al Knight shift in pure aluminum metal diminishes rapidly below the superconducting temperature²⁰ implying that it is dominated by the Fermi contact contribution. The ^{27}Al Knight shift in our dilute Ti base alloys is quite small, only about 0.03%, which is less than one-fifth of its value (0.164%) in pure Al. We interpret this small and positive ^{27}Al Knight shift to mean that the local s -electron density at the Fermi surface is small. When we include consideration of K_{ax} , to be discussed later, we find that this possibility is likely.

So far, we have considered only the isotropic Knight shift, but the line shape we observed contained structure characteristic of other nucleus-electron interactions. The data for Ti-V alloys at 29 MHz show evidence of an axially symmetric anisotropic Knight shift K_{ax} ; the two bumps on the low external field side of the absorption derivative show that K_{ax} is positive, i.e., $K_{\parallel} - K_{\perp} = 3K_{\text{ax}} > 0$. This is not surprising in view of the Ti-V phase diagram:⁸ at room temperature, for the concentration range of interest here, the equilibrium alloy structure is hcp and the vanadium atoms have axially symmetric local surroundings.

Table III lists the axially anisotropic Knight shift K_{ax} for several pure metals with hcp crystal structure and also for vanadium and aluminum in Ti-V and Ti-Al alloys. The list is in order of increasing c/a ratio. The dipolar interaction between nuclear and conduction-electron spins can give rise to this well-known anisotropic component of the Knight shift. In powders, this interaction will produce a characteristic asymmetry and broadening of the NMR line because of the isotropic distribution of crystal orientations present. This axially anisotropic Knight shift due to electron-dipolar interaction can be expressed as²¹

$$K_{\text{ax}}^{\text{dip}} \equiv 2 \left\langle \int \psi^* (3z^2 - r^2) r^{-5} \psi dV \right\rangle_{F\chi_p}, \quad (3)$$

where χ_p is the Pauli spin susceptibility and the integral is averaged over those electrons at the Fermi surface.

TABLE III. The anisotropic Knight shift K_{ax} and the c/a ratio of several pure hcp metals and of vanadium and aluminum in our Ti-V and Ti-Al alloys, respectively. All the K_{ax} values are measured at room temperature, unless noted.

Metal	c/a	K_{ax}	Note
Be	1.567	$< 0.0003\%$ ^a	
Y	1.571	-0.026% ^b	
Ti-1 (or 2) at. % Al	1.588	$\pm 1.5 \times 10^{-3} (\pm 0.5 \times 10^{-3})\%$	
Ti-1 (or 2) at. % V	1.588	$(0.029 \pm 0.001)\%$	
	1.588	$(0.039 \pm 0.001)\%$	77 K
Sc	1.597	-0.023% ^b	
		-0.030% ^c	77 K
		-0.032% ^c	4 K
Mg	1.623	0.0002% ^d	(Probably not known to within $\pm 0.0002\%$)
hcp spheres	1.633		
Cd	1.886	0.016% ^e	

^aW. T. Anderson, Jr., M. Ruhlig, and R. R. Hewitt, Phys. Rev. **161**, 293 (1967).

^bR. G. Barnes, F. Borsa, S. L. Segal, and D. R. Torgeson, Phys. Rev. **137A**, 1828 (1965).

^cReference 23.

^dG. C. Carter, L. H. Bennett, and D. J. Kahn, *Progress in Materials Science* (Pergamon, Oxford, 1977), Vol. 20, p. 247.

^eT. J. Rowland, Phys. Rev. **103**, 1670 (1956).

The quantity K_{ax}^{dip} is proportional to the deviation of the spatial distribution of Fermi-surface electrons from spherical (or, with tensor constraints, cubic) symmetry. For V in Ti, localized d electrons no doubt contribute to the observed K_{ax} value. Comparison with K_{ax} values of some other pure hcp metals can be made using Table III. Both beryllium and magnesium have a smaller c/a value than that of a hcp lattice of spheres, 1.633. The two metals have a free-atom outer structure of $2s^2$ and $3s^2$, respectively. A theoretical calculation²² for Be shows that in spite of substantial p character at the Fermi surface, the conduction-electron distribution is essentially isotropic and gives an extremely small K_{ax} .

Because of the d -orbital contribution to the field at nuclei in transition metals, Eq. (3) cannot be expected to describe the total observed K_{ax} . Narath¹¹ developed a theory of spin-lattice relaxation in hcp crystals that predicts a field orientation dependence of the orbital contribution to the relaxation rate; an orbital susceptibility anisotropy is also predicted. We consider two contributions to K_{ax} , namely, the orbital contribution K_{ax}^{orb} and the spin-dipolar contribution K_{ax}^{dip} . For the axial component of the anisotropic Knight shift caused by the unfilled d orbitals we have

$$K_{ax}^{\text{orb}} = 2 \langle r^{-3} \rangle_d \left[\frac{1}{3} (\chi_c^{\text{orb}} - \chi_a^{\text{orb}}) \right] N_0^{-1}, \quad (4)$$

where $\langle r^{-3} \rangle_d$ is averaged over all occupied states of the d band, χ_c^{orb} and χ_a^{orb} are the orbital susceptibilities per mole when the crystal c axis is parallel and perpendicular, respectively, to the external magnetic field, and N_0 is the number of atoms per mole.²³

From Table III, the two pure transition metals Y and Sc, which have negative K_{ax} values, have a c/a ratio smaller than 1.633. Cadmium, which has a positive K_{ax} value, has a c/a ratio larger than 1.633. For our alloys, with V or Al as a dilute impurity in Ti, the K_{ax} value at the solute site is very different from those in the above pure metals; they are also quite different from each other. There is no clear correlation with c/a alone. The K_{ax} value of the active nucleus depends upon the electronic structure of its total local environment.

For dilute Ti-Al and Ti-V alloys, the c/a ratio is the same while the K_{ax} value is very different. Considering first the Ti-Al alloys, the magnitude of K_{ax} at an Al site is about 0.0015% (the sign could not be determined from our experimental results); for the simple metal Al in Ti, the K_{ax}^{dip} term is expected to dominate K_{ax} . In view of the band structure of Ti, it seems (a) that the density of states of p character at the Fermi surface is small, and/or (b) that the Al p states are either partially full and isotropically occupied, or are full. In view of the magnitude of the K_{iso} of ²⁷Al in Ti, alternative (a) is favored.

For pure titanium, the anisotropy of the magnetic susceptibility $\chi_c - \chi_a$ was found to be 26.49×10^{-6} emu/mol.²⁴ The proportion of orbital and spin paramagnetic susceptibility in each direction is not known. But the average orbital susceptibility is found by Collings and Ho²⁴ to be 2.5 times the spin susceptibility. The latter is estimated by them using the electronic specific heat. In addition, they suggest that χ^{orb} is responsible for the

magnetic anisotropy of hcp Ti. We use their findings in interpreting our dilute ⁵¹V in Ti data.

We have no solid information regarding χ_c^{orb} and χ_a^{orb} in Ti or Ti-V alloys; however, assuming they have the same sign, we will then have a positive value for K_{ax}^{dip} . Several factors will contribute to a positive K_{ax}^{dip} value at the V site: the first is the charge shift of the interplanar bonding electrons, which are closer to the vanadium ion than the electrons on the basal plane. The V ion core has one more positive charge than the surrounding titanium. The interplanar charge for $c/a < (\frac{8}{3})^{1/2}$ may thus be drawn closer to the vanadium ion. A second possibility which would lead to a positive K_{ax}^{dip} is a bonding electron density between hcp planes which is greater than that in the basal plane. If K_{ax}^{dip} is positive, we can proceed with the analysis of our ⁵¹V measurements.

The bulk susceptibilities χ , χ_c^{orb} , and χ_a^{orb} of our dilute Ti-V alloys are expected to be approximately the same as those of pure titanium. Assuming the same proportion of orbital and spin paramagnetism exists in the average susceptibility and in χ_a and χ_c , we will have $\chi_c^{\text{orb}} - \chi_a^{\text{orb}}$ about 2.5 times that contributed by spin susceptibility. The $\chi_c^{\text{orb}} - \chi_a^{\text{orb}}$ will have a value of about 18.9×10^{-6} emu/mol. In order to estimate a K_{ax}^{orb} value for V by using Eq. (4), we need the value of $\langle r^{-3} \rangle_d$ for vanadium in hcp Ti. A crude estimate of $\langle r^{-3} \rangle = 1.6 \times 10^{25} \text{ cm}^{-3}$ has been made in Sec. IV A; using that value for $\langle r^{-3} \rangle_d$ for V($3d^5$) in Ti, a K_{ax}^{orb} value of 0.03% is obtained. This is in reasonable agreement with experiment (0.029%; see Table III).

For pure metallic Ti and Sc the same increase ($\sim 13\%$) (Refs. 17 and 18) in susceptibility and anisotropy $\chi_c - \chi_a$ has been found as temperature decreases from 298 to 77 K. At liquid-nitrogen temperature, the anisotropic Knight-shift value for ⁵¹V in a Ti matrix is 0.039%, which is about 30% larger than its room-temperature value. An increase of 30% in the magnitude of K_{ax} has been found also for ⁴⁵Sc in Sc in going to liquid-nitrogen temperature.²³ For Ti-V alloys, the small decrease in the lattice parameter (about 0.2% for both c and a values²⁵) and the unchanged c/a ratio²⁵ as temperature drops from 298 to 77 K indicates an increase of only about 0.6% in K_{ax}^{orb} . The use of bulk values in making this estimate is admittedly open to question. If we have an increase of d -electron density of states on the Fermi surface at liquid-nitrogen temperature, the K_{ax}^{dip} term will increase; it is not likely that n_i and n_f of Eq. (2) will undergo such a large change, likewise $\langle r^{-3} \rangle$. The 30% change seems to require a substantial change in d character; this could result from the Fermi energy lying near a peak in the density-of-states curve, thus producing a high $dN_d(E)/dT$ at E_F .

B. Electric-field gradient

The evaluation of the EFG even in a pure metal at a particular nuclear site remains in an unsatisfactory state, especially for group III, IV, and V transition metals (such as Sc, Ti, Y, Zr, and Hf).²⁶ This is because of the local d contribution, which the conduction-electron charge shift

model²⁷ does not take into account. The EFG computation is more difficult at a solute nucleus: a change in the solute outer electron wave function must occur when the solute is placed in the solvent matrix. Frequently, the total EFG at a nuclear site i in a noncubic metal host is assumed to result from the sum of the EFG due to the host lattice ions $q_{\text{ion}}[1-\gamma_{\infty}(i)]$ and the EFG attributable to the non- s character of the conduction electrons, i.e.,

$$q_i = q_{\text{ion}}[1-\gamma_{\infty}(i)] + q_{\text{non-}s} \quad (5)$$

The quantity $[1-\gamma_{\infty}(i)]$ is the Sternheimer antishielding factor²⁸ for the (solute) nucleus i at the site under discussion, and q_{ion} is the EFG which would exist at that point as a result of the ions of the lattice treated as point charges and summed over all sites other than i . Das and Pomerantz²⁹ have calculated the q_{ion} value for a particular c/a ratio to be

$$q_{\text{ion}} = (Z/a^3)[0.0065 - 4.3584(c/a - 1.633)] \quad (6)$$

The most stable valence of the host metal element is used for Z . For a dilute solid solution we approximate the EFG at a solute site using Eq. (5) and the $(1-\gamma_{\infty})$ value of the solute atom. The electronic part $q_{\text{non-}s}$ includes the contribution from the conduction- (outer) electron distribution; the wave functions for all of the occupied electron states are required for its evaluation.

The experimentally obtained q values at the solute site for our Ti-V and Ti-Al alloys are $\pm 7.2 \times 10^{23} \text{ cm}^{-3}$ and $\pm 4.4 \times 10^{23} \text{ cm}^{-3}$, respectively; these were found using nuclear quadrupolar moment $Q_{51} = -0.052 \times 10^{-24} \text{ cm}^2$ and $Q_{27} = 0.149 \times 10^{-24} \text{ cm}^2$.³⁰ The experimental q values are listed in column 2 of Table IV. The sign could not be determined by our technique. From Eq. (6), we can calculate the q_{ion} value for both Ti-V and Ti-Al alloys, which have a c/a ratio of 1.588. By using $Z=4$ for titanium ions, we obtain a q_{ion} value at V or Al in α -Ti of $3.15 \times 10^{22} \text{ cm}^{-3}$. The q_{ion} values are listed in column 3

of Table IV. The antishielding factors of the solute ions with ionization level of +5, +3, and +4 for V, Al, and Ti, respectively, are listed in column 4. The product of columns 3 and 4 is listed in column 5, which is the lattice component of the EFG. The conduction- (non- s) electron component of the EFG is calculated using Eq. (5) together with our experimental results from column 2; the result is listed in column 6 of Table IV. Column 7 lists the ratio of $q_{\text{non-}s}$ to $q_{\text{ion}}(1-\gamma_{\infty})$. From the ratio, we can see that a significant contribution to the EFG at V nuclei in Ti comes from electrons in the conduction band; this is also true for Al in Ti-Al. Ernst *et al.*³¹ found that the ratio of $q_{\text{non-}s}$ to $q_{\text{ion}}(1-\gamma_{\infty})$, let us call it A , is approximately equal to +2 for the group IIIb and IVb pure metals and about -3 for the group VIIb, VIIIb, and IIB pure metals. Hagn, Zahn, and Zech³² have measured the EFG at the solute site for many different solutes in Lu and in Re as host matrix. They found that in their alloys the sign of the EFG is fixed uniquely by the properties of the host, while the magnitude of $q_{\text{non-}s}$ appeared to depend linearly on the number of solute outer (s and d) electrons. They find no "universal correlation" relating the experimentally determined EFG data in quantitative detail. Let us assume the total EFG value at a V site in α -Ti, and at a Sc site in α -Ti, has the same sign since the sign relationship is found to be true for almost all impurity-host combinations.³³ We then have at room temperature about the same A value for V (with five outer electrons) and Sc (with three outer electrons), but an A value for Al which differs from that of Sc in the Ti host lattice: Al and Sc have the same number of outer electrons. This argument shows that $q_{\text{non-}s}$ does not have a linear dependence on only the number of impurity outer electrons. The outer electronic configuration *in toto* must be considered. At best any rule should be expected to hold for the filing of a single l shell only. The different A value for V and Ta in Ti is no doubt a reflection of the very large Sternheimer factor for Ta together with the

TABLE IV. Values of q at the solute V, Al, Sc, and Ta sites in Ti and at Ti in pure Ti; all the q values are in units of 10^{23} cm^{-3} .

Probe nuclei	q_{expt}	$q_{\text{ion}} (Z=4)$	$1-\gamma_{\infty} (\text{solute})$	$q_{\text{ion}} (1-\gamma_{\infty})$	$q_{\text{non-}s}$	$q_{\text{non-}s}/q_{\text{ion}} (1-\gamma_{\infty})$
⁵¹ V (298 K)	± 7.2	0.315	7.5 ^a	2.4	4.8 -9.6	2.0 -4.0
²⁷ Al (298 K)	± 4.4	0.315	3.59 ^b	1.13	3.3 -5.5	2.9 -4.9
⁴⁵ Sc (298 K)	$\pm 12.2^c$	0.315	14 ^d	4.41	7.8 -16.6	1.8 -3.8
¹⁸¹ Ta (298 K)	$\pm 37.8^e$	0.315	62 ^e	19.5	18.3 -57.3	0.9 -2.9
⁴⁹ Ti (1-4 K)	$\pm 8.1^f$	0.315	8.72 ^a	2.7	5.4 -10.8	2.0 -4.0
⁵¹ V (77 K)	± 8.4	0.315 ± 0.0079	7.5 ^a	2.4 ± 0.5	6.0 ± 0.5 -10.8 ± 0.5	2.5 ± 0.8 -4.5 ± 0.8

^aF. W. Langhoff and R. P. Hurst, Phys. Rev. **139A**, 1415 (1965).

^bP. C. Schmidt, K. D. Sen, T. P. Das, and A. Weiss, Phys. Rev. B **22**, 4167 (1980).

^cReference 29.

^dR. P. Gupta and S. K. Sen, Phys. Rev. A **8**, 1169 (1973).

^eReference 21.

^fReference 11.

^gThe uncertainty is the result of a variation in reported c/a ratios; see the text.

difference in bonding. V and Sc have the same core as Ti; the number of outer electrons differs by only +1 and -1, respectively. The fact that they have about the same A value emphasizes the importance of bonding in determining A . The q value at a Ti site in pure Ti at room temperature has not been measured, but q is expected to be nearly independent of temperature; for example, the q value of Sc in Ti shows no temperature dependence.³⁴ We presume the q value at a Ti site in pure Ti will probably be about the same at both room temperature and the measured value at liquid-He temperature.¹¹ One possible explanation for A having about the same value for V, Sc, and Ti in Ti (see Table IV) is that the outer electrons of V, Sc, and Ti bond nearly identically with their 12 nearest-neighbor Ti atoms. The one extra electron on V may possess predominantly s character, and in any case would act as a screening electron. Likewise, Sc would be expected to repel charge, but has a strong tendency to complete the bonding of the Ti structure and thus may promote s - to d -like orbitals.

We might anticipate that the A value of Al in a Ti host lattice would be different from that of V and Ti in a Ti host lattice. The neon core and the s - p character of the outer electrons are very different for Al. The spatially localized charge near an Al solute atom should be expected to differ radically in distribution from that of the Ti host. A recent work of Blaha, Schwarz, and Dederichs³⁵ using first-principles calculations to estimate the electric-field gradient in hcp metals showed that the EFG was determined mainly by the nonspherical distribution of the valence-electron density close to the nucleus, predominantly from p electrons. This is the case even for hcp transition metals, where the d anisotropy is large. From Table IV we note that the absolute value of A for Al in Ti is larger than that for either V in Ti or Sc in Ti; this implies a larger $q_{\text{non-}s}$ component for Al in Ti than that for either V in Ti or Sc in Ti. Considering the fact that V and Sc are transition elements and Al is a simple metal, the larger $q_{\text{non-}s}$ component for Al in Ti suggests that the contribution of p electrons to the EFG at an Al site is larger than the contribution of d electrons to the EFG at either a V or Sc site in a Ti matrix. (For V and Sc there are no unfilled p states.) Our experimental results support the conclusions of Blaha, Schwarz, and Dederichs³⁵ for a pure hcp metal.

At liquid-nitrogen temperature, the experimentally determined value of q at a V site in a Ti-V alloy is $\pm 8.4 \times 10^{23} \text{ cm}^{-3}$, which is about 17% higher than the room-temperature value. An increase in q as temperature decreases has been found for some other solutes in titanium, for example, Ta and Cd.^{36,37} The change in q for Ta in Ti and Cd in Ti is about 3% and 13%, respectively, in the temperature range 77–298 K. Precise point-charge lattice sums cannot be made for these systems because of the variation among the reported measurements of the anisotropy of thermal expansion in Ti metal. The lattice parameters a and c have been measured in the temperature region from 20 to 200°C and at some higher temperatures.^{20,32,33} Extrapolating these results to liquid-nitrogen temperature, c/a ratios of 1.587,³⁸ 1.588,²⁵ and 1.589 (Ref. 39) result from different studies. Using these

values for the c/a ratio at 77 K, we find the quantity $q_{\text{ion}}(1-\gamma_{\infty})$ for V (77 K) listed in Table IV. The almost constant value of $q_{\text{ion}}(1-\gamma_{\infty})$ suggests that the increase in q_i as temperature drops from 298 to 77 K is the result of an increase in the $q_{\text{non-}s}$ component. There is a 25% increase in the non- s contribution assuming q_{ion} and $q_{\text{non-}s}$ have the same sign, or a 12% increase if they have the opposite sign.

Forker and Krusch⁴⁰ and Kolk⁴¹ found that the electronic (non- s) contribution to q_i is roughly proportional to (or at least strongly related to) the density of states at the Fermi surface. Our data lead to an increased density of states at the Fermi surface when the temperature is decreased from 298 to 77 K according to their findings.

C. Field-independent line broadening.

The Gaussian broadening used in simulating the V absorption curve is about three times larger than the calculated pure dipolar width (the latter is approximately 1.0 Oe). Symmetric, field-independent line broadening is increased by dislocations and solute-solute nearest- or next-nearest-neighbor pair contributions to width. The latter also contribute to small distributions in the major interactions. At the highest external field strength, field inhomogeneity over the sample volume contributes about 0.5 Oe to the line broadening.

D. Effect of concentration

Referring again to the computer simulation described briefly in Sec. III A, a better fit was found for Ti-1 at. % V than Ti-2 at. % V resonance lines. The two experimental curves observed at 29 MHz are shown in Fig. 1. The two peaks on the low-field side of the Ti-1 at. % V resonance line are not present in the Ti-2 at. % V resonance line. The peaks are clearly present in the simulation (Fig. 2, 29 MHz). We base an interpretation of these facts on the following arguments applicable at 29 MHz. There are more V-V nearest-neighbor pairs for Ti-2 at. % V than Ti-1 at. % V. The probability that there are one or more vanadium atoms in the nearest-neighbor shell of a vanadium atom is approximately $1 - (1 - C_V)^{12}$, which is 0.215 (or 0.114) for a Ti-2 at. % V (or Ti-1 at. % V) alloy. The V-V nearest neighbors will give rise to isotropic and anisotropic Knight shifts different from an isolated V in Ti; a nonaxial anisotropic Knight shift will also arise. At lower frequencies, the experimental high-field-peak to low-field-peak ratio was larger than the simulated values for Ti-2 at. % V. For Ti-1 at. % V, the ratio was approximately the same as calculated. The proportion of V-V nearest-neighbor pairs may also be the reason for the ratio discrepancy at the lower frequencies.

E. Effect of annealing

Figure 3 shows the effect of annealing on the ⁵¹V resonance line shape at 29 MHz in the 1 at. % V alloy. Before annealing the alloy, the observed line (Fig. 3, top) had its higher positive going peak at the lower field. This shape cannot be simulated by a smooth, bell-shaped, continuous distribution of isotropic Knight shift, anisotropic

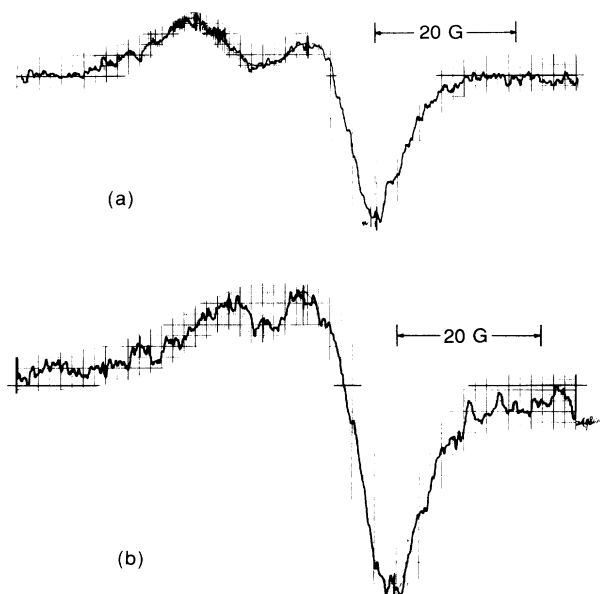


FIG. 3. The room-temperature, 29-MHz, experimental ^{51}V resonance line of the Ti-1 at. % V alloy (a) before and (b) after annealing. Magnetic-field calibration is shown; field increases to the right.

Knight shift, or a combination of the two. (Quadrupole effects are negligible at this field.)

A likely origin of the line shape at the top of Fig. 3 is the internal strain resulting from filing. Using the same 1 at. % V alloy for x-ray diffraction as for NMR analysis, about two times broader x-ray-diffraction peaks were obtained for the unannealed filings; this confirmed the presence of highly strained material and indicated a high density of dislocations. The strain field accompanying the dislocations perturbs both K_{iso} and K_{ax} through the sizeable lattice displacement and conduction-electron redistribution.

Powder samples were annealed at $\sim 0.5T_m$ in order to ensure recovery and yet avoid sintering of the particles. After annealing, the effect of dislocations on the solute vanadium resonance was reduced drastically. It was the

^{51}V resonance line in the annealed filings (Fig. 3, bottom) which could be reasonably well simulated. Similar annealing effects were observed for the Ti-2 at. % V alloy.

V. CONCLUSIONS

Very small isotropic and anisotropic Knight shifts were observed for ^{27}Al in Ti. This implies the absence of an orbital contribution and a very small value for the s conduction-electron density at the local Fermi surface in the vicinity of Al in Ti. On the contrary, vanadium, when present as a dilute solute in Ti, appears to share the Ti lattice charge distribution fully. A sizable isotropic and anisotropic Knight shift were observed for ^{51}V in Ti. We argue that this is the result of a large orbital contribution. The substitutional vanadium retains much of the electron configuration of V in metallic V, but is subject to the crystal field of the Ti lattice. Four outer electrons of V may form nearest-neighbor bonds similar to those between Ti atoms in pure titanium. The extra electron on the V may be more s -like in character. Measurement of the temperature dependence of K_{ax} and EFG values at V solute atoms in a Ti matrix show that both K_{ax} and EFG increase as temperature decreases. In band model language, the Fermi energy may lie near a peak in the density-of-states curve, in addition the density of states at E_F must increase with decreasing temperatures. A better explanation depends on a dependable localized model. The local electric-field-gradient contribution from non- s -electrons $q_{\text{non-}s}$ is about two to five times larger than the q_{ion} values in magnitude. Because the sign of the EFG is not determined, the validity of the so-called "universal correlation" could not be tested.

ACKNOWLEDGMENTS

We thank Professor E. Oldfield and Ben Montez for assisting us in the use of the superconducting magnet pulsed spectrometer system in the Chemistry NMR Facility. This research was supported in part by the U. S. Department of Energy under Contract No. DE-AC02-76-ER01198 through the Materials Research Laboratory of the University of Illinois at Urbana-Champaign. In addition, the work was supported by the Department of Metallurgy and Mining Engineering.

*Present address: Department of Materials Science and Engineering, National Tsing Hua University, Hsinchu 30043, Taiwan, ROC.

¹E. A. Stern, *Phys. Rev. B* **1**, 1518 (1970).

²M. Shimizu, T. Takahashi, and A. Katsuki, *J. Phys. Soc. Jpn.* **18**, 1192 (1963).

³E. A. Stern, *Phys. Rev.* **157**, 544 (1967).

⁴E. W. Collings, A. C. Ho, and R. I. Jaffee, *Titanium Science and Technology* (Plenum, New York, 1973), p. 831.

⁵T. J. Rowland and F. Borsa, *Phys. Rev.* **134**, A743 (1964); E. von Meerwall and T. J. Rowland, *Phys. Rev. B* **5**, 2480 (1972).

⁶R. G. Barnes, F. Borsa, S. L. Segal, and D. R. Torgeson, *Phys. Rev.* **137**, A1828 (1965).

⁷D. R. Torgeson and R. G. Barnes, *Phys. Rev.* **136**, A738 (1964).

⁸J. L. Murray, *Bull. Alloy Phase Diagrams* **2**, 48 (1981).

⁹P. M. Hansen, *Constitution of Binary Alloys*, 2nd ed. (McGraw-Hill, New York, 1958), p. 140.

¹⁰W. H. Jones, T. P. Graham, and R. G. Barnes, *Phys. Rev.* **132**, 1898 (1963).

¹¹A. Narath, *Phys. Rev.* **162**, 320 (1967).

¹²R. Watson and A. Freeman, *Phys. Rev.* **123**, 2027 (1961).

¹³L. H. Bennett, R. E. Watson, and G. C. Carter, *J. Res. Natl. Bur. Stand., Sec. A* **74A**, 569 (1970).

¹⁴M. H. Cohen, D. A. Goodings, and V. Heine, *Proc. Phys. Soc. London Sec. A* **73**, 811 (1959).

¹⁵J. Bardeen, L. N. Cooper, and J. R. Schrieffer, *Phys. Rev.* **108**, 1175 (1957).

¹⁶K. Yosida, *Phys. Rev.* **110**, 769 (1958).

- ¹⁷R. G. Barnes, F. Borsa, S. L. Segal, and D. R. Torgeson, *Phys. Rev.* **137**, A1830 (1965).
- ¹⁸A. Narath, *Phys. Rev.* **162**, 320 (1967).
- ¹⁹A. J. Freeman and R. E. Watson, *Magnetism* (Academic, New York, 1965), Vol. IIA, p. 290.
- ²⁰R. H. Hammond and G. M. Kelly, *Phys. Rev. Lett.* **18**, 156 (1967).
- ²¹G. C. Carter, L. H. Bennett, and D. J. Kahn, *Progress in Materials Science* (Pergamon, Oxford, 1977), Vol. 20, p. 63.
- ²²P. Jena, S. D. Mahanti, and T. P. Das, *Phys. Rev. Lett.* **20**, 544 (1968); **20**, 977(E) (1968).
- ²³J. W. Ross, F. Y. Fradin, L. L. Isaacs, and D. J. Lam, *Phys. Rev.* **183**, 645 (1969).
- ²⁴E. W. Collings and J. C. Ho, *Phys. Rev. B* **2**, 235 (1970).
- ²⁵W. T. Roberts, *J. Less-Common Met.* **4**, 345 (1962).
- ²⁶A. Maio, L. Hermans, M. Rots, G. N. Rao, and R. Coussement, *Hyper. Int.* **11**, 239 (1981).
- ²⁷E. Bodenstedt and B. Perscheid, *Hyperf. Int.* **5**, 291 (1978).
- ²⁸R. Sternheimer, *Phys. Rev.* **84**, 244 (1951).
- ²⁹T. P. Das and M. Pomerantz, *Phys. Rev.* **123**, 2070 (1961).
- ³⁰G. H. Fuller and V. W. Cohen, *Nucl. Data Tables* **5**, 508 (1969).
- ³¹H. Ernst, E. Hagn, E. Zech, and G. Eska, *Phys. Rev. B* **19**, 4460 (1979).
- ³²E. Hagn, M. Zahn, and E. Zech, *Phys. Rev. B* **28**, 3130 (1983).
- ³³R. S. Raghavan, E. N. Kaufmann, and P. Raghavan, *Phys. Rev. Lett.* **34**, 1280 (1975).
- ³⁴R. C. Reno, R. L. Rasera, and G. Schmidt, *Phys. Lett.* **50A**, 243 (1974).
- ³⁵P. Blaha, K. Schwarz, and P. H. Dederichs, *Phys. Rev. B* **37**, 2792 (1988).
- ³⁶E. N. Kaufmann, *Phys. Rev. B* **8**, 1387 (1973).
- ³⁷E. N. Kaufmann, P. Raghavan, R. S. Raghavan, K. Krien, and R. A. Naumann, *Phys. Status Solidi B* **63**, 719 (1974).
- ³⁸R. H. Willens, *Rev. Sci. Instrum.* **33**, 1069 (1962).
- ³⁹R. R. Pawar and V. T. Deshpande, *Acta Crystallogr. Sec. A* **24**, 316 (1968).
- ⁴⁰M. Forker and K. Krusch, *Phys. Rev. B* **21**, 2090 (1980).
- ⁴¹B. Kolk, *J. Phys. (Paris) Colloq.* **37**, C6-355 (1976).